Interaction of two oscillating sonoluminescence bubbles in sulfuric acid

Rasoul Sadighi-Bonabi,[1,*] Nastaran Rezaee,[1,2] Homa Ebrahimi,[1] and Mona Mirheydari[1,2]
[1]*Department of Physics, Sharif University of Technology, 11365-91 Tehran, Iran*
[2]*Department of Physics, Islamic Azad University Central Tehran Branch, Tehran, Iran*
(Received 24 February 2010; revised manuscript received 29 May 2010; published 29 July 2010)

The mutual interaction of two oscillating gas bubbles in different concentrations of sulfuric acid is numerically investigated. A nonlinear oscillation for spherical symmetric bubbles with equilibrium radii smaller than 10 μm at a frequency of 37 kHz in a strong driving acoustical field $P_a=1.8$ bar is assumed. The calculations are based on the investigation of the secondary Bjerknes force with regard to adiabatic model for the bubble interior which appears as repulsion or attraction interaction force. In this work the influence of the various concentrations of sulfuric acid in uncoupled and coupled distances between bubbles has been investigated. It is found that the sign and value of the secondary Bjerknes force depend on the sulfuric acid viscosity and its amount would be decreased by liquid viscosity enhancement. The results show that big change in the parameters of produced bubbles occurs in the sulfuric acid with concentrations from 65% to 85%.

DOI: 10.1103/PhysRevE.82.016316 PACS number(s): 78.60.Mq, 43.35.Ei

I. INTRODUCTION

Sonoluminescence (SL) is the production of picosecond light pulses from a collapsing bubble which is trapped in various liquids by a high amplitude ultrasound field [1]. This phenomenon is called single bubble sonoluminescence (SBSL) [2]. Different characteristics of such an interesting phenomenon are studied including intensity and spectrum of the emitted light [3–6], its dependency to the ambient parameters [7–9], dissolved gas in the liquids [10], phase diagrams [11–14], pulse width [15–17], conditions of bubble stability [18,19], and modification of the initial Rayleigh-Plesset equation considering various effects such as compression viscosity of the liquids [20,21]. Recently, the effect of thermal conductivities of various noble gases on sonoluminescence temperature has been studied [22]. The light intensity resulted from collapsing bubbles in sulfuric acid is 2700 times more than the production from water at the room temperature presented by Hopkins *et al.* in 2005 [23]. This has motivated the sonoluminescence researchers to investigate the radiative bubbles from similar environments [23]. In 2009 Moshaii *et al.* studied the radiation produced from a stable SBSL in different concentrations of sulfuric acid [24].

The other phenomenon which has been on the focus of the sonoluminescence researchers is moving SBSL [14,25] and it is shown that the components of the hydrodynamic force on an oscillating bubble are the reason of translational movement of a bubble in a trajectory [14,26]. Another attractive subject is the simultaneous SL radiation from several bubbles that is called multibubble sonoluminescence (MBSL) [27–33]. As a scientific analysis of MBSL, Mettin *et al.* investigated the mutual interaction force between two bubbles for different pressure amplitudes in water by considering the nonlinear oscillations of the bubbles [28]. In nonlinear resonance oscillation model the Rayleigh-Plesset equation governs the bubble's behavior under the periodic excitation characterized by the slow expansion and rapid collapse [28,29]. Yasui showed that in MBSL, the range of the ambient bubble radius diminishes as the ultrasonic frequency increases [30–32]. Ida *et al.* carried out some investigation of multibubble model including the observation of cavitation bubbles in liquid mercury [33]. In 2007 Eddingsaas and Suslick reported 95% sulfuric acid as a very suitable host liquid to investigate spectrum of Ar emission from the MBSL; they also noticed the influence of the acoustic power on the MBSL spectra of sulfuric acid [34]. Although in the above mentioned works very useful information about the MBSL has been produced, the interaction force between two bubbles, considering their nonlinear oscillations, except for the initial work on water [28], has never been discussed.

In this work the secondary Bjerknes force between two bubbles is investigated for coupled and uncoupled distances in different concentrations of sulfuric acid (resulting in different viscosities) with regard to the nonlinear radial oscillations for cavitations' bubbles. Based on the present calculations it is found that the liquid viscosity and bubbles' distance between two centers have the main roles in the interaction force, where the secondary Bjerknes force would be decreased by liquid viscosity enhancement. The magnitude of the interaction force would be increased by distance decrement, although the area for the repulsive force in the phase space of $R_{10}-R_{20}$ decreases when bubbles become closer. It must be noted that the area for the repulsive force in the phase space of $R_{10}-R_{20}$ (white area in Figs. 1 and 2) is the result of nonlinear oscillation of two bubbles.

It is found that the secondary Bjerknes force is decreased by viscosity enhancement; therefore, we would have an open cluster and more active bubbles to produce more intense emission from a cluster [35]. This is why one expects the higher intensity of light flashes from the MSBL at higher concentrations.

II. MODEL

The mutual interaction between two bubbles in MBSL, which is called the secondary Bjerknes force discovered by Bjerknes [28,30,36,37], is different from the primary

*sadighi@sharif.ir

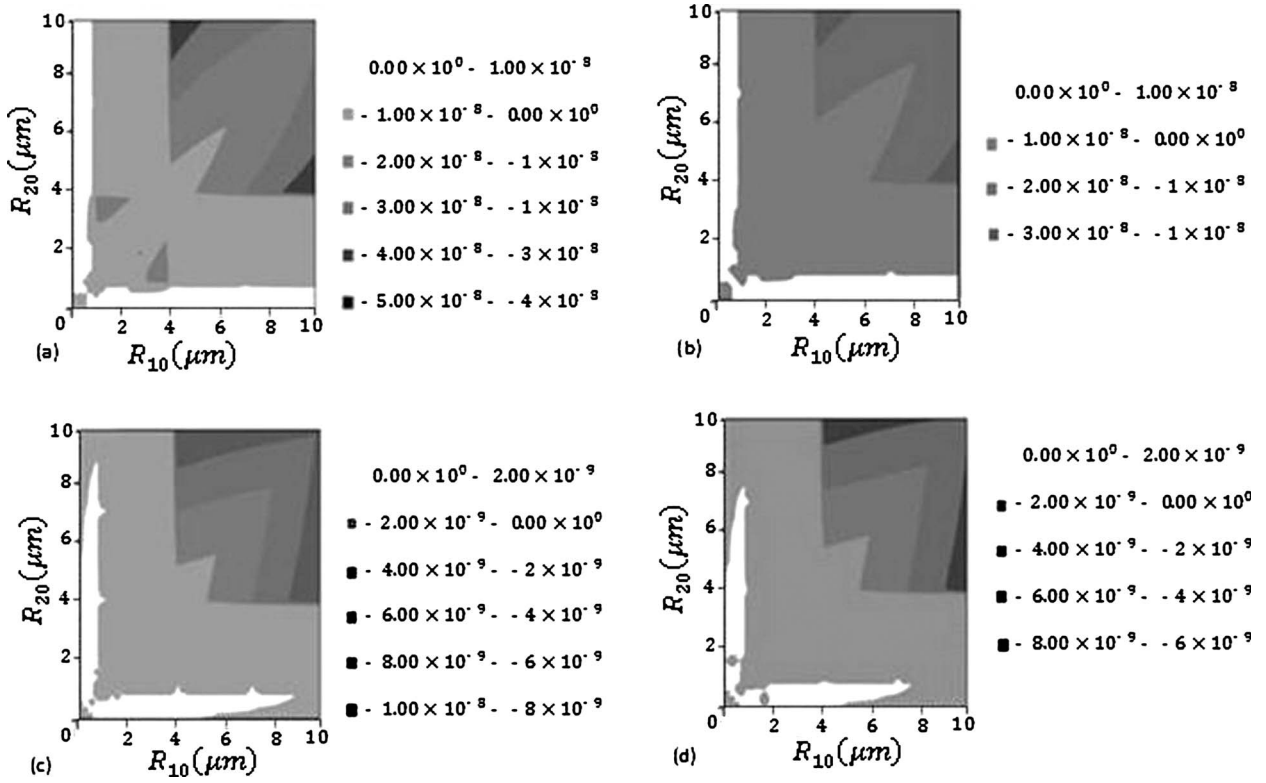

FIG. 1. The secondary Bjerknes force for the ambient radii of the first and the second bubbles, R_{10} and R_{20}, in size range smaller than 10 μm at the pressure amplitude of 1.8 bar for the uncoupled distance ($d=1$ cm) in four concentrations of sulfuric acid: (a) 45%, (b) 65%, (c) 85%, and (d) 95%. As it is shown the secondary Bjerknes force decreases as the viscosity increases.

Bjerknes force. The primary Bjerknes force is the exerted force on a bubble (at the pressure node or antinode of a stationary sound field) due to the pressure gradient of fluid [28,38]. The main reason of the formation of these forces is the acoustic pressure gradient [28].

To explain the coupled dynamics of two bubbles the Rayleigh-Plesset equation is applied for mutual interaction of two bubbles [28,39,40]. The wavelength of the sound field is large compared to the bubbles' distance and the bubbles' radii [28]. The bubbles are set to simultaneous oscillations in the same amplitude and phase as long as the spherical shapes of two bubbles are preserved. The velocity field $u_i(r,t)$ is as follows [28,39]:

$$u_i = \frac{R_i^2 \dot{R}_i}{r^2}, \tag{1}$$

where r, and $R_i(t)$ and $R_j(t)$ are the distance from a point in flask to the center of the first oscillating bubble, and the first and the second bubbles' radii, respectively.

The pressure gradient applied on each bubble is resulted from the driving pressure (primary Bjerknes force) and the effect of the neighboring bubbles (secondary Bjerknes force). The pressure gradient field is the source of the secondary Bjerknes force, and if the bubbles distance is small enough, the driving pressure of the bubbles would not be equal to the external driving pressure. The reason is the amplitude of the neighboring bubbles' oscillations, which cannot be neglected. Therefore, the pressure field represents an additional driving pressure for the second bubble [28,39,41–44]. In this work the bubbles are supposed to be far enough from each other, so the additional pressure would not disturb the spherical shape of the other bubble severely.

To calculate the pressure exerted on the second bubble by the first one, Euler equation (the equation of liquid flow) is used,

$$\rho \frac{\partial u_i}{\partial t} + \frac{\partial P_i}{\partial r} = 0, \tag{2}$$

where ρ and P_i are the density of the liquid and the pressure field radiated from the first bubble, respectively. The complete form of the Euler equation is

$$\frac{\partial u_i}{\partial t} + u_i \frac{\partial u_i}{\partial r} = -\frac{1}{\rho}\frac{\partial P_i}{\partial r}, \tag{3}$$

where u_i is the velocity field of the ith bubble in the $\hat{r}$ direction. In Eq. (3), the second term is negligible, because $u_i \partial u_i / \partial r$ is on the order of r^{-5} and it is much smaller than the first term [28].

Substituting Eq. (1) into Eq. (2) for the pressure exerted by the first bubble to the second one yields

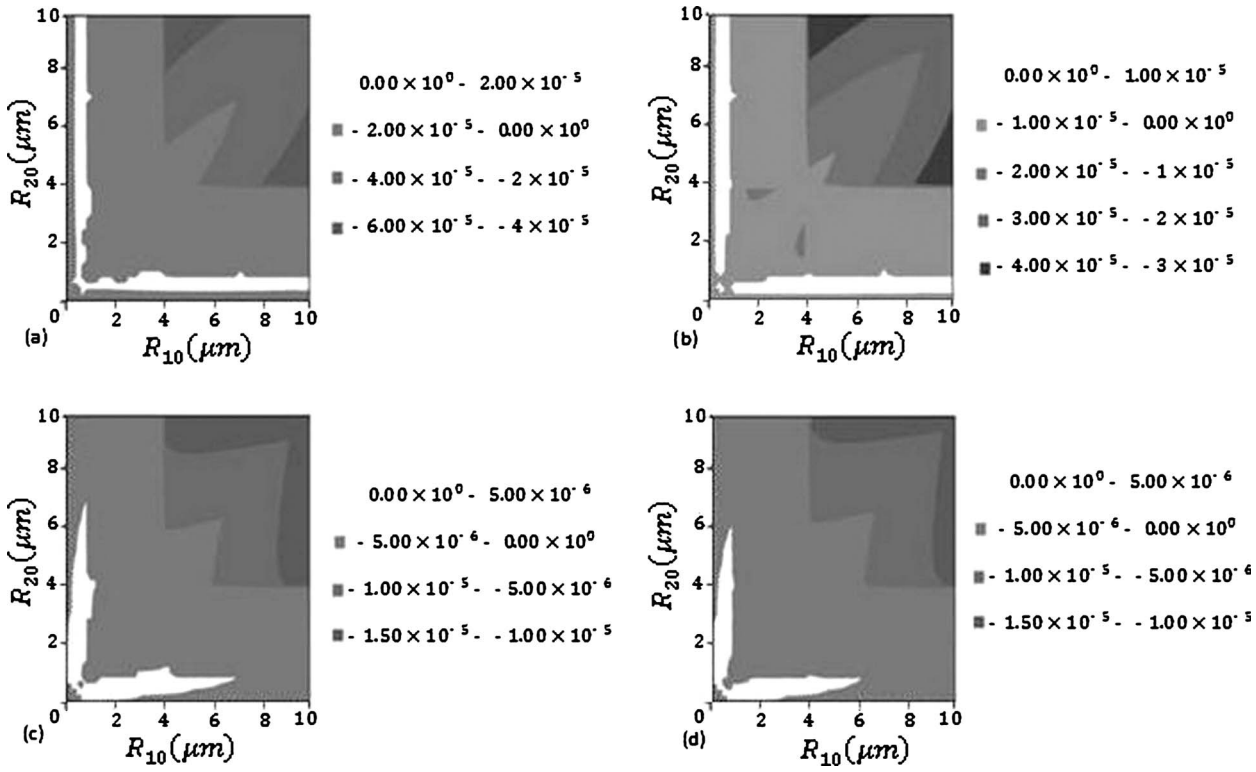

FIG. 2. Observation of the secondary Bjerknes force for the ambient radius of the first bubble R_{10} and the ambient radius of the second bubble R_{20} in the range of smaller than 10 μm at the pressure amplitude of 1.8 bar for the coupled distance (d=0.2 mm) in four concentrations of sulfuric acid: (a) 45%, (b) 65%, (c) 85%, and (d) 95%. As it is shown in the figures (legend box), the secondary Bjerknes force decreases by increasing of the viscosity.

$$P_i = \frac{\rho}{r}\frac{d}{dt}(R_i^2\dot{R}_i). \tag{4}$$

The secondary Bjerknes force exerted on the second bubble under a pressure gradient ∇P_i with volume v_j is

$$F_{ij} = -v_j \nabla P_i, \tag{5}$$

$$F_{ij} = -v_j\frac{\partial P_i}{\partial r}|_{r=d}e_r = v_j\frac{\rho}{d^2}\frac{d}{dt}(R_i^2\dot{R}_i)e_r = \frac{\rho}{4\pi d^2}v_j\frac{d^2v_i}{dt^2}e_r. \tag{6}$$

Here, d, v_i, and e_r are the distance between bubbles' centers, the volume of the first bubble, and the radial unit vector directed from the first bubble toward the second one, respectively. The definition of the secondary Bjerknes force F_B, which is the net radiation force from each bubble acting on its neighboring bubble in a sound field [28], is obtained from integration of Eq. (6) over a period of the volume oscillations,

$$F_B = \langle F_{ij}\rangle = -\frac{\rho}{4\pi d^2}\langle\dot{v}_i\dot{v}_j\rangle e_r = -\frac{f_b}{d^2}e_r, \tag{7}$$

where $\langle\dot{v}_i\dot{v}_j\rangle$ and f_b denote the time average of the bubbles' volume variations and secondary Bjerknes coefficient. The dynamics of the bubbles has a nonlinear model based on the Keller-Miksis equation [28,39,45], which describes the radial motion of a spherical bubble in a compressible liquid [28,46,47]. Using P_i from Eq. (4) and eliminating the high-order terms, similar to the procedure proposed by Mettin *et al.* [28], the equation for the second bubble is as follows:

$$\left(1-\frac{\dot{R}_j}{c}\right)R_j\ddot{R}_j + \left(\frac{3}{2}-\frac{\dot{R}_j}{c}\right)\dot{R}_j^2 = \frac{1}{\rho}\left(1+\frac{\dot{R}_j}{c}\right)P_{s,j} + \frac{R_j}{\rho c}\frac{d}{dt}P_{s,j} - \sum_{i=1,i\neq j}^{N}\frac{1}{D_{ij}}\frac{d(R_i^2\dot{R}_i)}{dt}. \tag{8}$$

Here i, j, and D_{ij} represent the first bubble, the second bubble, and the distance between two bubbles, respectively. In order to calculate the equation for the second bubble with regard to the secondary Bjerknes force, the influence of the first bubble oscillation on the second one should be considered; the last term on the right-hand side of Eq. (8) denotes the acoustical mutual force between the bubbles, which couples the equations of bubbles 1–N [39]; $P_{s,j}$ is obtained by considering a quasiadiabatic compression of an ideal gas within each bubble,

$$P_{s,j} = \left(P_{stat}+\frac{2\sigma}{R_{j0}}\right)\left(\frac{R_{j0}^3-h_j^3}{R_j^3-h_j^3}\right)\gamma - \frac{2\sigma}{R_j} - \frac{4\mu}{R_j}\dot{R}_j - P_{ex}(t) - P_{stat}, \tag{9}$$

TABLE I. Properties of sulfuric acid as a host liquid for trapped bubbles in different concentrations of sulfuric acid.

Sulfuric acid (wt %)	45	65	85	95
ρ (kg/m^3)	1347.6	1553.3	1778.6	1833.7
μ (cP)	3.18	6.9	25.08	26.59
σ (mN/m)	70.344	62.91	56.025	53.24
C (m/s)	1640	1631	1522	1439.69

where R_{j0}, P_{stat}, γ, σ, h_j, and μ are the equilibrium radius of the second bubble, static pressure, polytropic exponent (which switches between isothermal and adiabatic compressions), surface tension, $h_j=8.86/R_{j0}$, and the viscosity of the liquid, respectively. $P_{ex}=P_a \sin(2\pi ft)$ is the exerted driving pressure. It is clear that to calculate the effect of the pressure field of the second bubble on the first one, indices $i \leftrightarrow j$ would be exchanged in Eqs. (8) and (9). The secondary Bjerknes force will be obtained by substituting the solution of Eq. (8) in averaging procedure of Eq. (7). The secondary Bjerknes force of both bubbles is symmetric, where $\langle F_{ji}\rangle=-\langle F_{ij}\rangle$ [28].

III. NUMERICAL RESULTS

In this work, the secondary Bjerknes force F_B is calculated for two bubbles. At collapse time the wall velocity is high, so the mass and heat transfer are negligible; therefore, the adiabatic model would be a good model to interpret the gas evolution of the bubble interior. During the whole cycle of bubble's oscillation except for the collapse time, the interior bubble evolution follows the isothermal model [2,48,49]; thus, the quasiadiabatic model is applied. It is assumed that the bubbles have radii smaller than 10 μm, in different concentrations of sulfuric acid including 45%, 65%, 85%, and 95% at a pressure amplitude of $P_a=1.8$ bar and at 37 kHz driving frequency. In Table I, other parameters including μ, σ, ρ, and c, which were described before [50], are shown for various concentrations of sulfuric acid. From Table I one can notice that as the concentration of sulfuric acid increases, the viscosity is also increased. In the present work, the influence of the viscosity on the behavior of the bubbles is considered where the evolution of the bubble interior is assumed to be a quasiadiabatic model [48,49,51].

For detailed investigation of effects of the secondary Bjerknes force effect on each bubble's behavior including oscillating radius and wall velocity along with the secondary Bjerknes force diagram for specific size of the bubble are considered. In order to explain the influence of the interaction force between two bubbles, a bubble behavior is studied individually during 1 cycle, in different situations such as different fluid concentrations and different distances between the two bubbles, which is comparable to the work of Mettin *et al.* [28] with bubble size ranging from 0.2 to 10 μm. The behavior of two bubbles is observed in two states: coupled (0.2 mm distance between two bubbles) and uncoupled (1 cm distance between two bubbles).

According to the presence of $1/d^2$ factor in the F_B formula, where the bubbles become closer to each other, the secondary Bjerknes force increases (see Figs. 1 and 2). f_b is the Bjerknes force coefficient which is shown in Eq. (7). If the Bjerknes coefficient is positive ($f_b>0$), the interaction force F_B would be negative and it is known as attraction force, and if the Bjerknes coefficient is negative ($f_b<0$), the interaction force F_B would be positive and shows repulsion force between two bubbles. In Figs. 1 and 2 the region of attraction corresponds to the light and dark gray regions, which refer to the weak and strong secondary Bjerknes force attraction, respectively, and the white region refers to the repulsion between the bubbles. When the gray region becomes darker the value of the secondary Bjerknes force increases which indicates a strong attraction force between the bubbles.

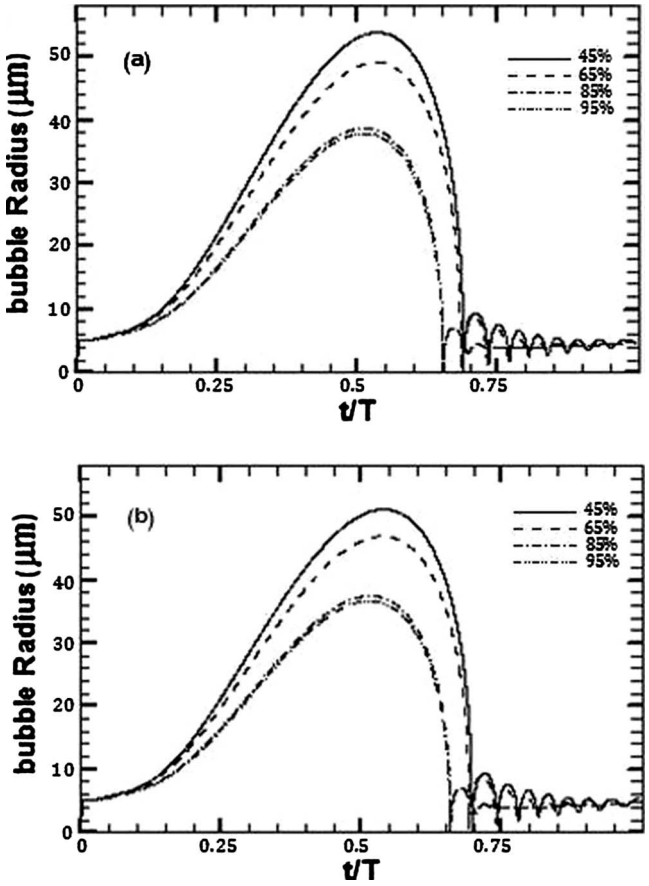

FIG. 3. Bubble radius R_1 vs normalized t/T during one driving period at pressure amplitude of 1.8 bar for $R_{20}=R_{10}=5$ μm for states (a) uncoupled=1 cm and (b) coupled=0.2 mm, in four different concentrations of sulfuric acid. In both figures the variation of maximum radius for concentrations from 65% to 85% is noticeable.

In Fig. 1, the secondary Bjerknes forces for two bubbles are compared in four concentrations of sulfuric acid in uncoupled state. The ambient radii of the two bubbles R_{10} and R_{20} vary between 0.2 and 10 μm. This figure shows that as the viscosity of sulfuric acid increases, the secondary Bjerknes force decreases and a strong attraction region which is denoted by darker gray, including a vast range of sizes for the bubbles' radii. The repulsion region occupies a smaller area by increasing the viscosity which is determined by

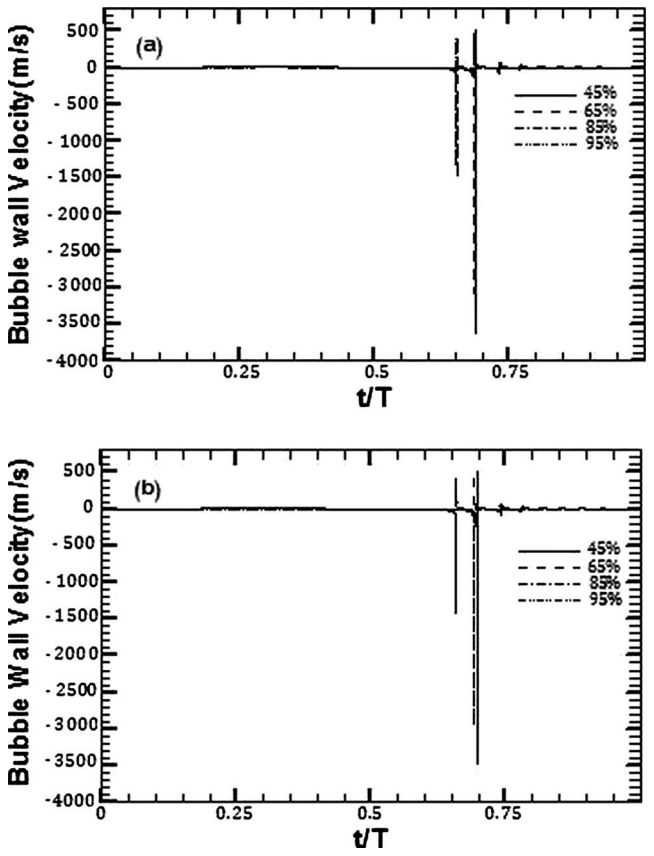

FIG. 4. Bubble wall velocity vs normalized t/T during one driving period at pressure amplitude of 1.8 bar for $R_{20}=R_{10}=5$ μm for states (a) uncoupled=1 cm and (b) coupled=0.2 mm in four different concentrations of sulfuric acid. As one can see, similar to the previous Figs. 1–3, in both figures the curves for concentrations of 45% and 65% almost coincide, where the same situation exists for the curves of concentrations of 85% and 95%. However, there is a big difference between the curves related to the concentrations of 65% and 85%.

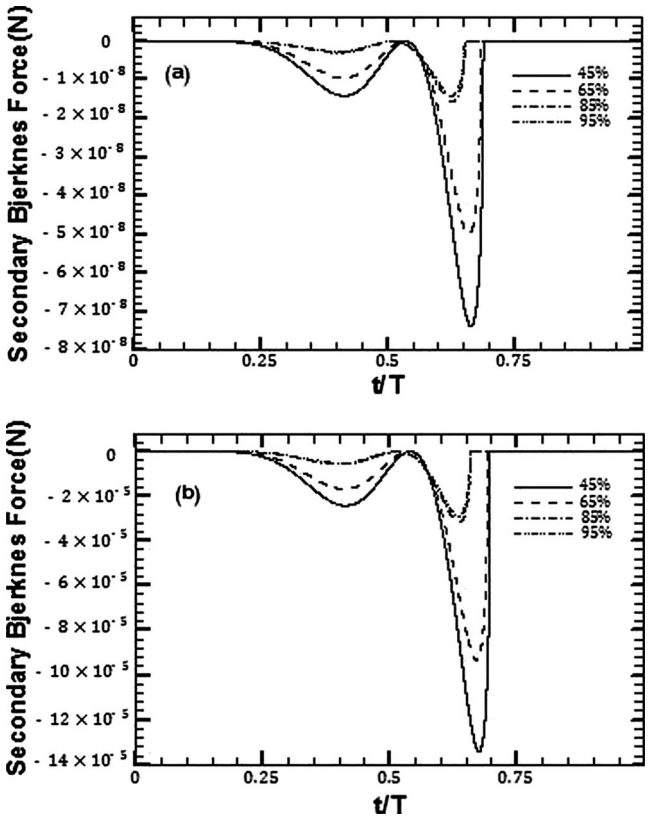

FIG. 5. Secondary Bjerknes force of the first bubble vs normalized t/T during one driving period at pressure amplitude of 1.8 bar for $R_{20}=R_{10}=5$ μm for states (a) uncoupled=1 cm and (b) coupled=0.2 mm in four different concentrations of sulfuric acid. The big gap can be seen for the plotted parameters between the 65% and 85% acid concentrations.

white color in the diagrams. It should be mentioned that for the bubbles which are completely different in size (one bubble is big and another one is small) in sulfuric acid with the highest concentration of 95%, the probability of the repulsion force (resulted from the nonlinear oscillations) decreases. By increasing the concentration the viscosity increases and the attraction region penetrates to the repulsion area. Generally, by viscosity enhancement, the influence of the nonlinear oscillation diminishes for two bubbles with big difference on their sizes. The variation of strong attraction force increases for the bubbles with bigger size ranges, especially for the bubbles which are in the range of 5–10 μm. It should be noticed that in acid with higher viscosity, the value of the secondary Bjerknes force is smaller.

Figure 2 shows the secondary Bjerknes force for different concentrations of sulfuric acid when the bubbles are in the coupled state. It is found that repulsion parts become thin and they occupy the areas where the bubbles have smaller sizes. It is obvious that, when the bubbles get closer, the bubbles would be attracted to each other with much higher interaction force. In addition to that, when the viscosity increases, the part related to the repulsion interaction force decreases in comparison to the uncoupled state, where the attraction part (gray color in Fig. 2) is increasing. Although the Bjerknes force decreases by increasing the viscosity, variation of the interaction force value increases from the uncoupled state to the coupled state in the gray color part, for the attraction force.

By comparing Figs. 1 and 2, one can see that the reduction in the repulsion area is more apparent in a liquid with higher viscosity (95% and 85%) than the liquid which has less viscosity. It means that in sulfuric acid with higher concentration, the reduction in the repulsion area becomes more obvious. The repulsion interaction part resulted from the nonlinear oscillation of the bubbles, decreasing in concentrations from 65% to 85%, considerably. The influence of the nonlinear oscillation does not have any remarkable decrement on the concentrations from 45% up to 65% and from 85% to 95%. Therefore, the variation of the white area in these concentrations can be neglected.

In Figs. 3–5 bubble behavior is investigated during 1 cycle for both coupled and uncoupled states. In this case, the influence of the viscosity on the bubbles behavior is studied. In order to cancel the effects of the nonlinear oscillation on the secondary Bjerknes force, two bubbles are supposed to

TABLE II. The maximum of secondary Bjerknes value during one driving period at pressure amplitude of 1.8 bar for $R_{20}=R_{10}=5$ μm for states uncoupled=1 cm and coupled=0.2 mm.

Sulfuric acid (wt %)	45	65	85	95
Secondary Bjerknes force (N) uncoupled state	7.376×10^{-8}	4.978×10^{-8}	1.564×10^{-8}	1.412×10^{-8}
Secondary Bjerknes force (N) coupled state	1.343×10^{-4}	9.339×10^{-5}	3.182×10^{-5}	2.890×10^{-5}

be in the same size (5 μm); otherwise, for big differences in the bubble diameters, the secondary Bjerknes force would be varied in sign via the influence of the nonlinear oscillation. In these figures the behavior of bubble parameters including bubble wall velocity, bubble ambient radius, and the secondary Bjerknes force is investigated only by considering the effect of the viscosity for both coupled and uncoupled states. Both bubbles are considered to be in the area of the attraction force (darker gray area in Fig. 1). It should be reminded that both bubbles are assumed to have the same size and they show the similar behavior. Here, the variation of the first bubble's radius versus time is investigated.

In Fig. 3, the oscillating radius of bubble in both states uncoupled [Fig. 3(a)] and coupled [Fig. 3(b)] is shown in four different concentrations of sulfuric acid including 45%, 65%, 85%, and 95%. As the viscosity of the bubble increases, the maximum of the bubble radius would be decreased. This decrement was expected according to the reduction in the bubble ability to expand and collapse, which is resulted from the viscosity increment.

In Fig. 3(b), it is observed that in the coupled state the maximum of the bubble radius decreases to 50 μm, while in the uncoupled state the maximum of the bubble radius is about 52 μm. This increment shows the influence of the coupled oscillation of the bubbles in the coupled state, which results in a limitation in the bubble behavior, and reduces the bubble's freedom to oscillate. There is also a time delay at the collapse instant with enhancement of the liquid viscosity as a result of the coupled oscillation of the bubbles in comparison to the uncoupled state. Although, for the sulfuric acid concentrations from 45% to 65%, the maximum radius decreases, there is a large gap between the maximum radii in higher liquid viscosities which is more observable for concentrations of 65% and 85%. In addition, the delay in the collapse time for the acid concentration is even more distinct for concentrations of 65% to 85%.

In Fig. 4, wall velocity variation of bubble during 1 cycle for different liquid viscosities is shown in both states: uncoupled [Fig. 4(a)] and coupled [Fig. 4(b)]. The bubble wall velocity decreases at the collapse moment with viscosity enhancement and the maximum of the bubble wall velocity decreases when the bubble is in the coupled state. The bubble wall velocity decrement is remarkable in sulfuric acid with lower viscosity. When the bubbles come closer, the effects of coupled radial oscillations of two bubbles on a bubble's wall velocity decrease with increasing of the liquid viscosity.

As the viscosity of the bubble increases, the rate of the bubble collapse and the bubble expansion would be decreased consequently. As a result of Eq. (7), the secondary Bjerknes force is proportional to the bubbles' volume variations, and the bubble volume derivation is proportional to radius derivation, defined as the bubble wall velocity. Therefore, because the secondary Bjerknes force is proportional to the bubble wall velocity ($\dot{R}_{10}$ or $\dot{R}_{20}$), by reduction in the bubble wall velocity, the secondary Bjerknes force [according to Eq. (7), $F_B<0$] also decreases. The variation of the secondary Bjerknes force is shown in Fig. 5. The secondary Bjerknes force has two picks during one acoustical cycle of radial oscillation. The small pick refers to the fast expansion of the bubble in 0.25–0.5 of a cycle, which is shown in Fig. 3, and the second one, which is larger in value, denotes the bubble collapse instant. Considering the relation between the secondary Bjerknes force and the distance between the bubbles, the value of the interaction force is enhanced by decrement of the bubbles' distance. Then the magnitude of the secondary Bjerknes force in coupled state [Fig. 5(a)] is stronger than the uncoupled state [Fig. 5(b)]. Furthermore due to the highest amount of the secondary Bjerknes force in the 45% concentration, its variation is more obvious than other concentrations (Table II).

Based on the above mentioned figures, a firm reason can be deduced to show an inverse relation between the influence of the nonlinear oscillation of the bubbles and the liquid viscosity enhancement. In Figs. 1 and 2, the dependence on the bubble viscosity is shown for four different concentrations of sulfuric acid. In these figures, white region represents the effects of the nonlinear coupled oscillations of two bubbles in the various volumes.

IV. CONCLUSION

The behavior of two bubbles is studied in four different concentrations of sulfuric acid in uncoupled and coupled states. The observations show that the value of the secondary Bjerknes force decreases by viscosity enhancement and the area for the repulsive force in the phase space of $R_{20}-R_{10}$ decreases when the viscosity increases. In Figs. 1 and 2, the decrement of repulsion area is observable by the white part, which relates to the bubbles with big difference in their sizes.

From the presented results for 5 μm bubbles in Figs. 3–5 there are big differences between bubble parameters including bubble radius, bubble wall velocity, and secondary Bjerknes force, for sulfuric acid concentrations from 65% to

85%. In Figs. 1 and 2, the secondary Bjerknes force variation for big range of bubbles' sizes (0.2–10 μm) is considerable for sulfuric acid concentrations of 65% and 85%. However, the variation of similar parameters of the bubble for sulfuric acid concentrations from 45% to 65%, and also from 85% to 95%, is negligible.

ACKNOWLEDGMENTS

The authors acknowledge the research deputy of Sharif University of Technology for financial support of this project. We also thank Dr. E. Lotfi and Dr. L. Nikzad for their constructive comments.

[1] D. F. Gaitan and L. A. Crum, J. Acoust. Soc. Am. **91**, 3166 (1992).
[2] B. P. Barber, R. A. Hiller, R. Lofstedt, S. J. Putterman, and K. R. Weninger, Phys. Rep. **281**, 65 (1997).
[3] R. Hiller, S. Putterman, and B. P. Barber, Phys. Rev. Lett. **69**, 1182 (1992).
[4] W. C. Moss, D. B. Clarke, and D. A. Young, Science **276**, 1398 (1997).
[5] R. Hiller, S. Putterman, and K. Weninger, Phys. Rev. Lett. **80**, 1090 (1998).
[6] M. J. Matula, J. Guan, and L. A. Crum, Phys. Rev. E **64**, 026310 (2001).
[7] B. P. Barber, C. C. Wu, R. Lofstedt, P. H. Roberts, and S. J. Putterman, Phys. Rev. Lett. **72**, 1380 (1994).
[8] S. Hilgenfeldt, D. Lohse, and W. C. Moss, Phys. Rev. Lett. **80**, 1332 (1998).
[9] G. E. Vazquez and S. Putterman, Phys. Rev. Lett. **85**, 3037 (2000).
[10] R. Hiller, K. Weninger, S. Putterman, and B. P. Barber, Science **266**, 248 (1994); R. Hiller and S. Puterman, Phys. Rev. Lett. **75**, 3549 (1995).
[11] B. P. Barber, K. Weninger, R. Lofstedt, and S. Putterman, Phys. Rev. Lett. **74**, 5276 (1995).
[12] R. G. Holt and D. F. Gaitan, Phys. Rev. Lett. **77**, 3791 (1996).
[13] G. Simon, I. Csabai, A. Horvath, and F. Szalai, Phys. Rev. E **63**, 026301 (2001).
[14] R. Toegel, S. Luther, and D. Lohse, Phys. Rev. Lett. **96**, 114301 (2006).
[15] B. P. Barber, R. Hiller, K. Ariska, H. Fetterman, and S. Putterman, J. Acoust. Soc. Am. **91**, 3061 (1992).
[16] M. Moran and D. Sweider, Phys. Rev. Lett. **80**, 4987 (1998).
[17] R. Pecha, B. Gompf, G. Nick, Z. Q. Wang, and W. Eisenmenger, Phys. Rev. Lett. **81**, 717 (1998).
[18] M. P. Brenner, D. Lohse, D. Oxtoby, and T. F. Dupont, Phys. Rev. Lett. **76**, 1158 (1996).
[19] I. Akhatov, N. Gumerov, C. D. Ohl, U. Parlitz, and W. Lauterborn, Phys. Rev. Lett. **78**, 227 (1997).
[20] A. Moshaii and R. Sadighi-Bonabi, Phys. Rev. E **70**, 016304 (2004).
[21] A. Moshaii, R. Sadighi-Bonabi, and M. Taeibi-Rahni, J. Phys.: Condens. Matter **16**, 1687 (2004).
[22] A. Moshaii, R. Rezaei-Nasirabad, Kh. Imani, M. Silatani, and R. Sadighi-Bonabi, Phys. Lett. A **372**, 1283 (2008).
[23] S. D. Hopkins, S. J. Putterman, B. A. Kappus, K. S. Suslick, and Carlos G. Camara, Phys. Rev. Lett. **95**, 254301 (2005).
[24] A. Moshaii, Kh. Imani, and M. Silatani, Phys. Rev. E **80**, 046325 (2009).
[25] Yu. T. Didenko, W. B. McNamara III, and K. S. Suslick, Nature (London) **407**, 877 (2000).
[26] Rasoul Sadighi-Bonabi, Reza Rezaei-Nasirabad, and Zeinab Galavani, J. Acoust. Soc. Am. **126**, 2266 (2009).
[27] L. A. Crum, Phys. Today **47**(9), 22 (1994).
[28] R. Mettin, I. Akhatov, U. Parlitz, C. D. Ohl, and W. Lauterborn, Phys. Rev. E **56**, 2924 (1997).
[29] J. P. Franc and J. M. Michel, *Fundamentals of Cavitation* (Kluwer Academic Publishers, Dordrecht, 2004).
[30] V. F. K. Bjerknes, *Die Craftfelder* (Vieweg, Braunschweig, 1909).
[31] F. R. Young, *Sonoluminescence* (CRC Press, Boca Raton, FL, 2005).
[32] K. Yasui, J. Acoust. Soc. Am. **112**, 1405 (2002).
[33] M. Ida, T. Naoe, and M. Futakawa, Phys. Rev. E **75**, 046304 (2007).
[34] N. C. Eddingsaas and K. S. Suslick, J. Am. Chem. Soc. **129**, 3838 (2007).
[35] D. Sunartio, M. Ashokkumar, and F. Grieser, J. Phys. Chem. B **109**, 20044 (2005).
[36] C. A. Bjerknes, *Hydrodynamische Fernkrafte* (Engelmann, Leipzig, 1915).
[37] V. F. K. Bjerknes, *Fields of Force* (Columbia University Press, New York, 1906).
[38] L. A. Crum, J. Acoust. Soc. Am. **57**, 1363 (1975).
[39] M. Ida, T. Naoe, and M. Futakawa, Phys. Rev. E **76**, 046309 (2007).
[40] M. Ida, Phys. Rev. E **79**, 016307 (2009).
[41] M. Ida, Phys. Lett. A **297**, 210 (2002); J. Phys. Soc. Jpn. **71**, 1214 (2002).
[42] A. Ooi and R. Manasseh, ANZIAM J. **46**, C102 (2005) [http://anziamj.austms.org.au/V46/CTAC2004/Ooi1].
[43] M. Ida, Phys. Rev. E **72**, 036306 (2005).
[44] M. Ida, Phys. Fluids **17**, 097107 (2005).
[45] J. B. Keller and M. Miksis, J. Acoust. Soc. Am. **68**, 628 (1980).
[46] A. Prosperetti and A. Lezzi, J. Fluid Mech. **168**, 457 (1986).
[47] U. Parlitz, V. Englisch, C. Scheffczyk, and W. Lauterborn, J. Acoust. Soc. Am. **88**, 1061 (1990).
[48] M. P. Brenner, S. Hilgenfeldt, and D. Lohse, Rev. Mod. Phys. **74**, 425 (2002).
[49] R. Löfstedt, B. P. Barber, and S. J. Putterman, Phys. Fluids A **5**, 2911 (1993).
[50] L. Gmelin and R. J. Meyer, *Gmelins Handbuch Der Anorganischen Chemie* (Verlag Chemie GmbH, Leipzig, 1985).
[51] S. Hilgenfeldt, S. Grossmann, and D. Lohse, Phys. Fluids **11**, 1318 (1999).